

NP-BERT: A Two-Staged BERT Based Nucleosome Positioning Prediction Architecture for Multiple Species

Ahtisham Fazeel^{1,2}^a, Areeb Agha²^b, Andreas Dengel^{1,2}^c and Sheraz Ahmed¹^d

¹German Research Center for Artificial Intelligence, Kaiserslautern, Germany

²Department of Computer Science, Technical University of Kaiserslautern, Germany

Keywords: Nucleosome Position, DNA, Genomics, Language Models, Transformers, BERT, Masked Language Modeling, Transfer Learning.

Abstract: Nucleosomes are complexes of histone and DNA base pairs in which DNA is wrapped around histone proteins to achieve compactness. Nucleosome positioning is associated with various biological processes such as DNA replication, gene regulation, DNA repair, and its dysregulation can lead to various diseases such as sepsis, and tumor. Since nucleosome positioning can be determined only to a limited extent in wet lab experiments, various artificial intelligence-based methods have been proposed to identify nucleosome positioning. Existing predictors/tools do not provide consistent performance, especially when evaluated on 12 publicly available benchmark datasets. Given such limitation, this study proposes a nucleosome positioning predictor, namely NP-BERT. NP-BERT is extensively evaluated in different settings on 12 publicly available datasets from 4 different species. Evaluation results reveal that NP-BERT achieves significant performance on all datasets, and beats state-of-the-art methods on 8/12 datasets, and achieves equivalent performance on 2 datasets. The codes and datasets used in this study are provided in <https://github.com/FAhtisham/Nucleosome-position-prediction>.

1 INTRODUCTION

The organization of eukaryotic and prokaryotic life is generally controlled by the presence and accessibility of the genetic material inside the cells (Tsompana and Buck, 2014). The genetic material is usually very long and is compacted by the presence of specialized structures, nucleosomes. The nucleosome is the core and fundamental unit of chromatin polymer, which is formed by the combination of histone proteins and DNA (Luger, 2003). Usually, there are two copies of four different histones i.e., H2A, H2B, H3, and H4, around which the DNA is wrapped. To achieve a high degree of compactness and accessibility, 147-160 base pairs of DNA are wrapped around a core octamer of histones, whereas the sequences that are responsible to connect the nucleosomes are approximately 20-30 bp in length and are often referred to as linker sequences. Furthermore, nucleosomes are considered the first organizational layer

of the eukaryotic genome, which lays the foundation for chromatin fibers, topologically associated domains (TADs), and active or inactive compartments (Uljanov et al., 2016). A more comprehensive exploration of the eukaryotic genetic material suggests that the nucleosome positioning and higher-order chromatin structures act as control logic for DNA.

The packing of DNA around nucleosomes plays important role in various processes like DNA replication, genome expression, DNA repair, and transcription (Tsompana and Buck, 2014). Besides its direct involvement, the genome-wide location of nucleosomes is rudimentary for various biological processes. For example, gene regulation is one of the mechanisms that is influenced by its genome-wide positioning, as the binding of protein for transcription initiation is affected by the presence of nucleosomes. In addition, various studies have reported a plethora of diseases associated with abnormal histone modifications in the nucleosome structure, such as sepsis, autoimmune diseases, thrombosis, cerebral stroke, trauma, and tumors (Cho et al., 2004; Chen et al., 2014).

Multiple experimental approaches are used to identify or quantify nucleosome positioning,

^a  <https://orcid.org/0000-0002-7174-7676>

^b  <https://orcid.org/0000-0003-2827-4129>

^c  <https://orcid.org/0000-0002-6100-8255>

^d  <https://orcid.org/0000-0002-4239-6520>

such as chromatin immunoprecipitation sequencing (ChIP-Seq) (Schmid and Bucher, 2007), immunoprecipitation-chip (ChIP-chip) (Ozsolak et al., 2007), assay for transposase-accessible chromatin with high-throughput sequencing (ATAC-Seq) (Buenrostro et al., 2015), DNase-seq and FAIRE-seq, and MNase-Seq (Chereji and Clark, 2018). Due to the advent of next-generation sequencing methods, multiple high-resolution genome-wide nucleosome maps have been made available for multiple species, such as *Homo sapiens*, *Saccharomyces cerevisiae*, and *Caenorhabditis elegans* (Shtumpf et al., 2022). In spite of the availability of large-scale datasets, the determinants in the DNA sequences for nucleosome positioning are not yet fully characterized. To unveil such determinants and the understanding of nucleosome positioning multiple approaches have been proposed, yet more accurate tools/algorithms can prove helpful in exploring the phenomenon of nucleosome positioning, and the impact of gene mutations on nucleosomes.

Existing studies opted for machine or deep learning-based approaches to predict nucleosome positioning. Initially, a predictor iNuc-PseKNC was developed by Gou et al. for the classification of nucleosome positioning (Peckham et al., 2007). Authors converted discrete DNA sequences into statistical vectors by incorporating the frequency of different k -mers, ranging from $k=\{1, \dots, 6\}$, and trained a support vector machine (SVM) classifier on it. The predictor proposed by Gou et al. managed to produce a reasonable performance on the dataset of *Saccharomyces cerevisiae* (Shtumpf et al., 2022). Chen et al. proposed iNuc-PhysChem, where DNA sequences were first transformed into statistical vectors based on 12 different physiochemical properties. iNuc-PhysChem was evaluated against the genome of *Saccharomyces cerevisiae*. In addition, the extension of the work was done by incorporating deformation energy for the prediction of nucleosome positioning (Chen et al., 2016).

Cui et al. proposed a nucleosome positioning predictor namely, ZCMM (Cui et al., 2019). Authors converted raw DNA sequences into statistical vectors by incorporating Z-curve theory along with position weight matrix (PWM). In addition, ZCMM used SVM for classification of nucleosome positioning and was trained and evaluated on the genomes of 3 different species, i.e., *Homo sapiens* (HS), *Caenorhabditis elegans* (CE), and *Drosophila melanogaster* (DM). According to the performance evaluation of ZCMM, it showed significant performance only across the dataset of DM.

Gangi et al. proposed the deep learning predictor

DLNN, for the prediction of nucleosome positioning (Di Gangi et al., 2018). The predictor was based on one hot encoded sequence representation (OHE) for the conversion of DNA sequences into statistical vectors. The predictor proposed by them was based on convolution and long short-term memory neural networks. DLNN was the first predictor that was evaluated against 11 different datasets, belonging to diverse species i.e., *Homo sapiens* (HM), *Caenorhabditis elegans* (CE), *Drosophila melanogaster* (DM), and *Saccharomyces cerevisiae* (YS).

Zhang et al. proposed a deep learning-based predictor namely, LeNup (Zhang et al., 2018). LeNup made use of one hot encoding (OHE) to transform DNA sequences into a statistical vectors and performed classification by Google Inception and gated convolutional neural network. In addition, LeNup was evaluated on the genomic data of 4 different species i.e., HM, CE, DM, and YS. Amato et al. extended the idea of LeNup, and proposed another nucleosome positioning predictor CORENup (Amato et al., 2020). CORENup used OHE to represent DNA nucleotides and used convolution neural networks and long short-term memory units (LSTMs) for classification. CORENup was evaluated on 10 diverse types of benchmark datasets belonging to prior mentioned species.

Han et al. proposed another deep learning-based predictor namely, NP_CBiR (Han et al., 2022). NP_CBiR exploited the lack of use of long-range dependencies of the DNA nucleotides and designed a predictor that incorporated contextual information (embeddings) and nucleotide dependencies. The predictor was mainly based on two components, i.e. embedding part that leads to the contextual information and Bi-LSTM/Bi-GRU part that modeled the long-range nucleotide dependencies. In particular, NP_CBiR followed the core concepts of Gangi et al. (Di Gangi et al., 2018) to design a predictor that could perform consistently well across various nucleosome positioning datasets. NP_CBiR was evaluated on 10 similar datasets that were provided in the study of Gangi et al. (Di Gangi et al., 2018).

Taking into account the plethora of tools developed to predict nucleosome positioning, there are still some challenges in terms of predicting nucleosome positioning correctly. Firstly, existing predictors do not have consistent performance across all the benchmark datasets for nucleosome positioning. In addition, these methods showed lower performance and higher bias for positive and negative class samples. Considering these limitations, the idea of predicting nucleosome positioning is still considered crucial, and there is a need for more robust tools to predict

nucleosome positioning from the DNA sequences of various species.

By contemplating the prior mentioned limitations, the contributions of this study are multifarious and listed below;

- (I) We perform the classification of the benchmark datasets by utilizing various feature extraction methods, and a random forest (RF) classifier. Then, we reason for the limited performance of the statistical feature extraction methods by visualizing them into the feature space.
- (II) We pre-train and fine-tune the language model (BERT) on the datasets of nucleosome positioning in three different settings and perform evaluations on all the benchmark datasets.
- (III) In addition, we propose a two-staged fine-tuning mechanism for the pre-trained BERT model and perform evaluation across all nucleosome positioning datasets.
- (IV) We also present an ablation study to demonstrate the performance gains obtained through the two-stage fine-tuning as compared to single-stage fine-tuning and MLM pre-training settings.
- (V) Finally, we compare the performance of the proposed predictor (NP-BERT) with state-of-the-art methods for nucleosome position prediction, and evaluation results reveal that the proposed (NP-BERT) achieves superior performance over state-of-the-art methods across 8/12 datasets and shows equivalent performance on 2 datasets.

2 BACKGROUND

The working paradigms of various DNA feature extraction methods, transfer learning, BERT, and LSTM are briefly discussed in this section.

2.1 Feature Extraction Methods For DNA Sequences

Machine or deep learning models can not operate on textual data due to their inherent dependency on statistical vectors. Various DNA feature extraction methods are used to convert DNA sequences into numerical vectors by retaining useful information. These methods convert DNA sequences into statistical vectors by either computing the frequencies of nucleotides or physicochemical properties based on the correlation among nucleotides. DNA feature

extraction methods can be seen into three different categories i.e., mathematical, gap-based, and physiochemical properties-based methods (Chen et al., 2021) and PyFeat (Muhammod et al., 2019).

As DNA sequences are comprised of nucleotides, in the simplest way statistical representations of the DNA sequences are generated by computing the distribution of k-mers (a combination of nucleotides). Similarly, accumulated nucleotide frequency (ANF) generates statistical representations of the DNA sequences by computing position-specific densities of nucleotides. Pseudo-K-tuple nucleotide composition (PseKNC) incorporates the distribution of k-mers of various sizes to generate statistical representations of the DNA sequences.

Certain feature extraction methods rely on the occurrence frequencies of nucleotides, i.e., ATCG ratio, GC content. ATCG ratio generates 1-dimensional representations of DNA sequences, by computing the total occurrences of A and T, and then by normalizing them with the total occurrences of G and C. Similarly, GC content produces statistical representations by computing the ratio among total occurrences of nucleotides G and C to the total occurrences of all nucleotides. Cumulative skew is based on AT and GC skew, where AT skew is the ratio of the difference between total occurrences of A and T to the sum of their total occurrences, and GC skew can be computed in a similar way but with the occurrences of G and C nucleotides. A complex network follows the principle of word2vec algorithm, in which an undirected graph is constructed to represent the relations among the k-mers. Further, an adjacency matrix is generated and various topological measures are applied to generate statistical representations of the DNA sequence i.e., minimum degree (MIN), average short path length (ASPL), etc.

There are several other DNA feature extraction methods that also incorporate the gaps along with the k-mers of the DNA sequence i.e. gap k-mers A-G, and A-C, etc. Such methods work in a three-step process, first, a dictionary of the k-mers is generated for size k, then k-mers are generated from the original sequences. In the final step, by comparing and counting the k-mers with both of these dictionaries, statistical vectors are generated for DNA sequences. Such methods include MonoMonoKgap, MonoDiK-Gap, DiMonoKGap and so on which differ only in terms of k-mers sizes and the number of gaps.

Inspired by the chemical and biological properties of DNA nucleotides, different methods tend to encode such information in statistical vectors in an efficient manner. Such physiochemical properties include twist, roll, bend, hydrophobicity, electron-ion

potential, and polarity. The values of each nucleotide against each property have been computed experimentally and are provided in the literature. Electron interaction pseudopotentials (EIIP) transforms raw sequences into statistical vectors by supplanting each nucleotide with the pseudo-potentials specific float value. PseEIIP is an extension of EIIP that computes the mean distribution of free electron charge by generating 3-mers of the sequence and adding pseudopotentials for each nucleotide. The k-mers are first generated, then in each k-mer, the pseudopotential values corresponding to all nucleotides are added to represent the k-mers with their statistical properties.

In Dinucleotide based auto covariance (DAC), statistical vectors of DNA sequences are generated in 3 steps. First, pairs of nucleotides are generated on the basis of the lag value. Then two dinucleotide pairs are selected and physiochemical information is incorporated by taking the difference of dinucleotide pairs physiochemical values with the mean physiochemical values for all nucleotides. In the third step, such values are computed for all the nucleotide pairs and summed up, and then normalized with the difference in length of the sequence and lag value. In this way, for each physiochemical property, there is once a scalar value, and $N \times \text{LAG}$ dimensional vector is formed. Similarly, dinucleotide-based cross-covariance (DCC) follows similar steps and differs from DAC in one way. It compares two different physiochemical indexes for dinucleotides pairs. Furthermore, similar steps are modified along with some additional steps in other feature extraction methods such as, (TCC) and tri-nucleotide-based auto-cross covariance (TACC), Pseudo dinucleotide composition (PseDNC) and so on.

2.2 Transfer Learning

Transfer learning refers to the idea of using the information learned from a model developed for one task on a different yet related task. This leads to significant performance gains, and better generalization in spite of having a limited amount of training samples (Koumakis, 2020). Transfer learning can be done in two different ways i.e., supervised training, where a model is trained along with the labels, and unsupervised where the model is trained without the labels.

Formally, transfer learning considers a source domain $\mathcal{D}_S = \{X, P(X)\}$, and source task \mathcal{T}_S , a target domain $\mathcal{D}_T = \{X, P(X)\}$ and a target task \mathcal{T}_T . The objective of transfer learning is to learn the target conditional probability distribution $P(Y_T|X_T)$ from the target domain \mathcal{D}_T with the features learned from \mathcal{D}_S and \mathcal{T}_S .

2.3 Language Modeling and Bidirectional Encoder Representation From Transformers

For NLP tasks, word embeddings are commonly used from larger pre-trained models for classification purposes (Mikolov et al., 2013). Word embedding methods learn the contextual and syntactic relations of words in a defined contextual window. In particular, many word embedding methods are used, such as global vectors for word representations (Glove) (Sakketou and Ampazis, 2020), common bag of words (CBOW) (Word2vec and FastText), and skip-gram model. Prior mentioned methods can be seen in two main groups i.e., contextualized (W2vec), and non-contextualized (Glove). Moreover, the concept of self-attention and transformers opened new ventures for more accurate predictions for natural language tasks. The open-AI GPT model is based on the decoder of the transformers, yet the embeddings generated are just unidirectional (Floridi and Chiriatto, 2020). In comparison, BERT (Devlin et al., 2018) is only based on the encoders where multiple transformer encoders are stacked on each other, and the working paradigm of an encoder can be seen in 3 main steps. In the first step, word piece tokenization is done on the input sentence and then the input embedding is generated by incorporating three different embeddings namely, token and segment embeddings, and positional encoding. In token embeddings, each word or token is assigned a 768-dimensional vector. Segment embeddings are used in the next sentence prediction-based pre-training where the tokens belonging to the first sentence are assigned a 0 index and for the second sentence 1 is used. As BERT is able to process the whole sentence at once, therefore positional information related to each word is obtained by sinusoidal and cosine waves in order to fuse word order information. To learn the word associations, BERT utilizes the concept of multi-head attention where the first 3 different matrices are generated, query, key, and value. They are passed to a function such that attention filter could be learned, as shown in equation 1. This step is followed by a skip connection along with a layer normalization step and a feed-forward layer.

$$Attention(Q, K, V) = softmax\left(\frac{QK^T}{\sqrt{d_k}}\right)V \quad (1)$$

The pretraining of BERT is performed in an unsupervised or self-supervised manner in two different ways i.e., masked language modeling (MLM) and next-sentence prediction. In masked language modeling 15% of total tokens are masked in a sentence,

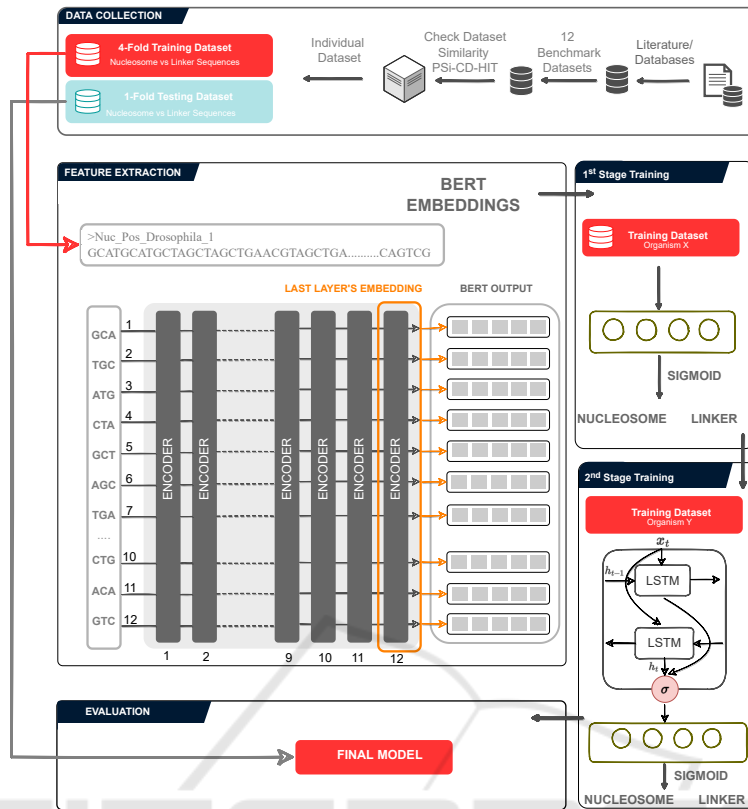


Figure 1: Overall methodology of the proposed study.

where out of total masked tokens 80% of the tokens are replaced with [MASK], 10% are replaced with a random token, and 10% tokens remain unchanged. Due to the efficient use of attention mechanisms and its training strategies, BERT obtained state-of-the-art results in multiple natural language tasks, such as speech recognition, text classification, question-answering, and text summarization.

Google AI has released multiple versions of BERT model, i.e., BERT-base with 12 encoder layers, 768 hidden units, and 12 attention heads. Similarly, BERT-large has 24 encoder layers, 1024 hidden units, and 16 attention heads. Similar models were used and pre-trained on the human genome by Ji et al, (Ji et al., 2021).

2.4 Long Short Term Memory (LSTM)

Long Short Term Memory (LSTMs) are a type of recurrent neural network (RNNs) that tackle the problems of long-range sequence dependencies in natural language data (Di Gangi et al., 2018). LSTMs are comprised of repeating units or cells, which contain three different gates, i.e., input gate, forget gate, and output gate (Yu et al., 2019). These gates are dependent on their inputs, and hidden states followed by a

non-linear activation i.e., tanh or sigmoid.

The forget gate receives the current input x_t , and hidden state of the previous LSTM unit h_{t-1} . This information is passed through a sigmoid function that assigns a higher probability to the information that is crucial and vice versa. Similarly, the input gate uses sigmoid function to keep the important and relevant information, followed by a tanh activation which normalizes the inputs into a range of -1 to 1. The addition of forget and input produce the hidden state of the LSTM unit h_t . The output gate is also comprised of sigmoid and tanh activation, where a point-wise multiplication is applied on the hidden state and normalized inputs. LSTM efficiently tackles the long-range dependency problem, by sharing the hidden and cell state information with its underlying units.

3 NP-BERT: THE PROPOSED APPROACH

Figure 1 shows the complete working paradigm of NP-BERT for nucleosome positioning prediction. NP-BERT is comprised of two main components i.e. a backbone and a head. The backbone is based

on a BERT model which is pre-trained on the human genome sequences with the length of the sequences between 5 and 510 with 3-mer of nucleotides. Whereas, in the head of the overall architecture, a bidirectional long short-term memory neural network or a fully connected layer is used for the classification.

First, 12 different benchmark datasets are collected from different sources and studies. Secondly, these datasets are passed through PSI-CD-HIT (Huang et al., 2010) to find the redundant sequences among all the datasets. The redundancy is checked in order to avoid any bias during the two-stage fine-tuning of NP-BERT. Then the datasets are encoded and passed through the BERT backbone which has 12 encoder layers, to obtain statistical representations. These representations are taken from the last encoder layer of BERT and passed through a classifier for the nucleosome positioning prediction. In this phase, a two-stage fine-tuning strategy is opted to increase the predictive capability of the model. The head of the overall setup changes at both steps of fine-tuning i.e., at the first stage a fully connected layer is used, and in the second stage LSTM and a fully connected layer are used in the head. The fine-tuning process of NP-BERT is illustrated in Figure 2.

The overall architecture is trained with a two-stage fine-tuning process. Consider, M as a pre-trained model, that has been already trained in an unsupervised manner on the DNA sequences of the human genome. We take a dataset, D_1 from the set of nucleosome positioning datasets and fine-tune the pre-trained model M on it, which can be considered the fine-tuned model M_1 for D_1 . We do fine-tuning of the pre-trained model M individually on all the nucleosome positioning datasets $D = \{D_1, D_2, \dots, D_{12}\}$ such that model M_1 is a fine-tuned model only on nucleosome positioning dataset D_1 , model M_2 is a fine-tuned model on nucleosome positioning dataset D_2 , and so on. This first fine-tuning produces 12 different models, i.e., $M = \{M_1, M_2, M_3, \dots, M_{12}\}$ that are fine-tuned on individual datasets separately.

At the second stage of fine-tuning, we take again a dataset D_i and 11 out of 12 fine-tuned-models such that the fine-tuned model M_i has not seen the nucleosome positioning dataset D_i . So for dataset D_1 , 11 models will be taken i.e., $M = \{M_2, M_3, \dots, M_{12}\}$. For D_1 , model M_1 is not taken as it is already fine-tuned on this dataset, and performing evaluation using this model will lead to biased results. Similarly, for D_2 , $M = \{M_1, M_3, \dots, M_{12}\}$ are taken and so on for the other datasets. At this point, these models are fine-tuned and evaluated once again. On the basis of maximum performance scores of various evaluation measures, a model is picked for that specific

dataset. For example, for dataset D_1 , out of 11 models $M = \{M_2, M_3, \dots, M_{12}\}$, M_3 leads to the maximum performance, thus it is considered the final model for that specific dataset. The same process is repeated for the other datasets which result in 12 models for nucleosome positioning datasets.

Table 1: A toy example of two-stage fine-tuning on the HM dataset.

Model	Dataset 1st-Stage	Dataset 2nd-Stage	Accuracy	AUC-ROC
G1				
M_1	DM	HM	83.94	91.13
M_2	CE	HM	88.33	94.41
M_3	HM	HM	Dropped	Dropped
M_4	YS	HM	87.59	94.40
G2				
M_5	DM-5UTR	HM	86.51	92.06
M_6	DM-LC	HM	50.0	54.86
M_7	DM-PM	HM	50.04	49.44
M_8	HM-PM	HM	87.77	92.88
M_9	HM-LC	HM	50.04	49.91
M_{10}	HM-PM	HM	50.04	56.41
M_{11}	YS-PM	HM	82.42	89.12
M_{12}	YS-WG	HM	50.04	50.0

To understand dual-stage fine-tuning, we incorporate an experimental example here over the dataset of the human genome (HS). Consider that we pre-trained a BERT-based model on the 3-mer of human genome sequences as mentioned earlier. This specific model is fine-tuned individually on the datasets of nucleosome positioning which produces 11 models, where the fine-tuned model on the HS datasets is discarded to avoid any bias and overfitting on HS dataset. All the models are passed through the second stage of fine-tuning where the models are fine-tuned and evaluated on the HS dataset. The performance of such models is shown in table 1 based on the accuracy and AUC-ROC values (for details see evaluation).

It can be seen from the table 1 that for dataset HM, fine-tuning is performed on 11 different datasets. Where among all the models and combinations of fine-tuning, the combination CE-HM yields maximum performance in terms of AUC-ROC and accuracy. To avoid any bias and overfitting from the model, similar datasets are not used in the 1st and 2nd stages of fine-tuning, which is also shown in the table 1, where the HM-HM combination is discarded.

3.1 Benchmark Datasets

In order to develop and evaluate nucleosome positioning predictors, several datasets have been developed in the existing studies (Di Gangi et al., 2018; Amato et al., 2020; Han et al., 2022). We have collected 12 different datasets from the study of Gangi et al. (Di Gangi et al., 2018). The datasets belong to 4 different species, i.e., *Homo sapiens* (HM), *Caenorhab-*

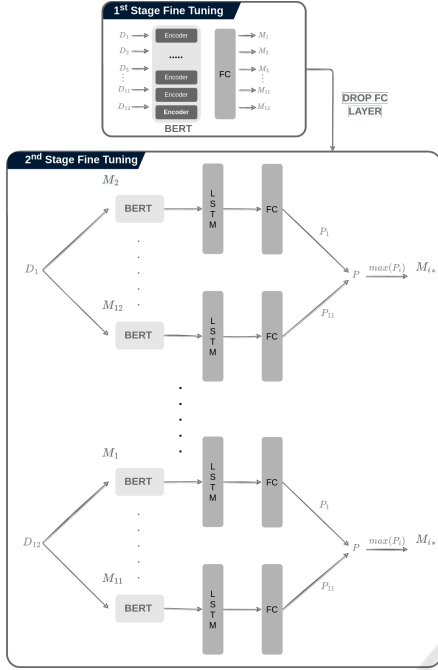


Figure 2: Fine-tuning strategy for the BERT model at two different stages.

ditis elegans (CE), *Drosophila melanogester* (DM), and *Saccharomyces cerevisiae* (YS).

The datasets are divided into two main groups i.e., G1, and G2. The first group has four datasets namely, HM, DM, CE, and YS. The statistics of the datasets from G1 are given in Table 2. The datasets of group 1 are balanced where the number of positive samples is close to the number of negative samples.

Table 2: Statistics of 4 different benchmark datasets from group 1.

Sequences	HM	DM	CE	YS
Positive	2273	2900	2567	1740
Negative	2300	2850	2608	1880
Total	4573	5750	5175	3620

The G2 contains 8 different datasets belonging to 3 species namely, *Homo sapiens* (HM), *Drosophila melanogester* (DM), and *Saccharomyces cerevisiae* (YS), and were originally developed by Liu et al. (Liu et al., 2014). Group 2 contains a variety of datasets from each specie, the largest chromosome (LC), promoter (PM) and 5' UTR exon region (5U) sequences from DM and HM, whole genome (WG), and promoter (PM) sequences of YS. The statistics of the datasets from G2 are given in table 3. The datasets in group 2 are highly imbalanced in nature which makes it more challenging to design a robust, and generalizable that can perform consistently on both sets of datasets. In addition, the datasets in group 1 and

2 have DNA sequences of 147 nucleotide bases, organized in two classes i.e., nucleosome forming sequences (positive) and nucleosome inhibiting linker sequences (negative).

Table 3: Statistics of 8 different benchmark datasets from group 2 belonging to three different species.

Sequences	HM			DM			YS	
	LC	PM	5U	LC	PM	5U	WG	PM
Positive	97209	56404	11769	46054	48251	4669	39661	27373
Negative	65563	44639	4880	30458	28763	2704	4824	4463
Total	162772	101043	16649	76512	77014	7373	44485	31836

3.2 Implementation Details and Hyper-parameters

The statistical DNA feature extraction methods are implemented in Python using iLearnPlus library (Chen et al., 2021). Machine learning classifiers are implemented by utilizing scikit-learn (Pedregosa et al., 2011). BERT-based models are also implemented in Python using the Pytorch library. Moreover, different hyperparameter combinations are used to find out the optimal set of hyperparameters, i.e., weight decay, epochs, and learning rate, for the training and fine-tuning of the BERT models at the first and second stages.

In the pre-training of BERT, the model is trained for 20000 steps with an attention dropout probability of 0.1, intermediate size 3072, layer normalization epsilon $1e^{-12}$, 12 attention heads in each BERT encoder, and embedding size 512. Adam is used as an optimizer with a weight decay of 0.01, beta 0.9, and 0.098 with a learning rate of $4e^{-4}$.

In the first fine-tuning stage, the models are trained with a batch size of 32, over 5 epochs with a learning rate of $2e^{-4}$ with a hidden dropout of 0.1, weight decay 0.01, and Adam is used as an optimizer. At the second stage of fine-tuning, the models are fine-tuned over a batch size of 32, along with a learning rate of $2e^{-5}$ with Adam as an optimizer across 3 epochs. In both of the fine-tuning stages, binary cross entropy is used as the loss function.

4 EVALUATION METRICS

Following the evaluation criteria of existing nucleosome positioning predictors, to evaluate and perform a performance comparison of the proposed predictor with existing nucleosome positioning predictors, we analyze the performance of the proposed predictor by using 5 different evaluation measures. i.e, accuracy (ACC), sensitivity (SN), specificity (SP), Math-

ews correlation coefficient (MCC), and area under the receiver operating characteristic (AU-ROC) (Amato et al., 2020; Han et al., 2022; Di Gangi et al., 2018).

ACC is the proportion of correctly predicted samples over all the predicted samples. SP is the fraction of truly predicted negative samples over all the predictions of the negative samples. Similarly, sensitivity (SN) is the ratio of the correct predictions made on the positive class samples to the sum of correct and false predictions made on the positive class samples. Area under receiving operating curve (AU-ROC) measures performance score using true positive and true negative rates calculated at various thresholds. Precision (PR) is the ratio of true predictions made on the positive class samples over all the positive predicted samples. MCC computes the performance score of a classification model, by considering the real and predicted classes of all the samples. The mathematical equations of aforesaid evaluation measures are given as,

$$f(x) = \begin{cases} \text{ACC} = (T_P + T_N) / (T_P + T_N + F_P + F_N) \\ \text{Specificity (SP)} = T_N / (T_N + F_P) \\ \text{Sensitivity (SN) or Recall (R)} = T_P / (T_P + F_N) \\ \text{Precision (P)} = T_P / (T_P + F_P) \\ \text{True Positive Rate (TPR)} = T_P / (T_P + F_N) \\ \text{False Positive Rate (FPR)} = F_P / (T_N + F_P) \\ \text{MCC} = \frac{T_P \times T_N - F_P \times F_N}{E} \\ E = \sqrt{(T_P + F_N)(T_P + F_P)(T_N + F_P)(T_N + F_N)} \end{cases} \quad (2)$$

5 RESULTS

This section briefly illustrates the performance of three different experimental settings of the BERT models and explains which setting produces the maximum performance for nucleosome positioning prediction. On the basis of maximum performance from these settings, we perform a comparative performance study of the proposed and existing approaches across 12 different nucleosome positioning datasets. In addition, this section comprehensively explains the performances of various DNA feature extraction methods and their intrinsic analyses across a randomly selected dataset from nucleosome positioning datasets.

5.1 Ablation Study

We categorize the experimentation of NP-BERT into three different settings i.e., i) NP-BERT (MLM Training) ii) NP-BERT (Single Stage), and iii) NP-BERT (Two Stage). An ablation study is then carried out to demonstrate the performance enhancements obtained through a two-stage fine-tuning of NP-BERT.

Table 4: Performance values of 3 NP-BERT settings over nucleosome positioning datasets.

Dataset/Species	Method	SN	SP	PR	ACC	MCC	AUC-ROC
Group 1							
CE	NP-BERT (MLM)	87.2	91.2	91.1	89.2	78.6	95.0
	NP-BERT (Single stage)	86.12	91.47	91.30	88.80	76.92	94.28
	NP-BERT (Two stage)	91.8	92.1	91.8	90.5	80.5	95.8
DM	NP-BERT (MLM)	79.2	87.5	86.4	83.5	67.2	90.9
	NP-BERT (Single stage)	84.8	84.9	84.9	84.8	69.9	92.9
	NP-BERT (Two stage)	84.8	85.6	85.3	85.1	70.5	92.4
YS	NP-BERT (MLM)	99.9	99.8	99.8	99.8	99.7	100
	NP-BERT (Single stage)	99.8	99.91	99.91	99.9	99.82	100
	NP-BERT (Two stage)	100	99.8	99.8	100	99.82	100
HM	NP-BERT (MLM)	79.3	86.8	86.5	83.1	66.9	91.4
	NP-BERT (Single stage)	90.30	86.59	87.12	88.01	69.09	91.17
	NP-BERT (Two stage)	88.3	88.4	88.5	88.3	76.8	94.4
Group 2							
DM-5U	NP-BERT (MLM)	33.7	91.0	74.8	69.9	33.0	68.7
	NP-BERT (Single stage)	42.2	84.9	62.6	69.2	30.4	68.2
	NP-BERT (Two stage)	41.1	85.8	63.8	69.5	30.8	68.3
DM-PM	NP-BERT (MLM)	40.5	93.4	78.4	73.6	40.5	73.2
	NP-BERT (Single stage)	47.0	88.0	71.6	72.7	39.7	72.2
	NP-BERT (Two stage)	40.1	93.6	80.4	73.6	42.0	73.7
DM-LC	NP-BERT (MLM)	33.9	95.2	82.7	70.8	38.5	71.6
	NP-BERT (Single stage)	48.2	85.5	69.0	70.6	36.8	71.3
	NP-BERT (Two stage)	43.1	90.0	75.2	71.3	38.7	72.0
HM-5U	NP-BERT (MLM)	35.3	95.7	78.7	78.0	41.5	75.2
	NP-BERT (Single stage)	55.4	92.3	75.4	81.0	52.8	80.0
	NP-BERT (Two stage)	51.6	94.3	80.0	81.8	53.4	80.2
HM-LC	NP-BERT (MLM)	71.8	96.6	93.4	86.6	72.5	91.7
	NP-BERT (Single stage)	85.4	94.4	91.2	90.8	80.8	94.8
	NP-BERT (Two stage)	83.7	96.1	93.7	91.1	81.7	95.1
HM-PM	NP-BERT (MLM)	70.2	89.8	84.4	81.1	61.8	86.6
	NP-BERT (Single stage)	74.5	91.5	87.0	83.5	69.0	89.6
	NP-BERT (Two stage)	75.8	92.4	89.1	85.1	70.1	90.4
YS-PM	NP-BERT (MLM)	53.0	89.7	84.9	91.5	62.5	92.3
	NP-BERT (Single stage)	61.3	97.6	81.1	92.4	66.0	93.1
	NP-BERT (Two stage)	63.1	97.2	79.6	92.4	66.3	93.5
YS-WG	NP-BERT (MLM)	62.1	96.6	71.1	92.8	61.7	92.3
	NP-BERT (Single stage)	62.0	97.6	77.4	93.0	65.3	93.7
	NP-BERT (Two stage)	60.3	98.4	82.7	94.3	67.2	94.5

5.1.1 NP-BERT (MLM Training)

The very first setting is comprised of a backbone of BERT model for extraction of statistical representations from the DNA sequences and the head is a linear or fully connected layer with a sigmoid function for the purpose of classification. Initially, the BERT backbone is trained in a self-supervised manner with masked language modeling. The training is done on the nucleosome positioning datasets, by combining all 12 benchmark datasets to form a larger and more appropriate dataset for BERT pre-training. After the pre-training, NP-BERT is then fine-tuned on the individual nucleosome positioning datasets and thus evaluated on the basis of 5-fold validation.

5.1.2 NP-BERT (Single Stage)

In the second setting, a pre-trained BERT is used to extract the statistical representations from the DNA sequences, coupled with a linear layer for the purpose of classification. The pre-trained DNABERT is then fine-tuned on the datasets of nucleosome positioning separately.

5.1.3 NP-BERT (Two Stage-Finetuning)

In the third setting, a pre-trained BERT model is fine-tuned in two different stages. In the very first stage, the model is fine-tuned on one dataset and in the second stage, it is fine-tuned and evaluated on the second dataset. Based on maximum performance such combinations are selected for further performance comparison and analyses.

Table 4 illustrates the performance scores across 6 different evaluation measures of three different NP-BERT settings on 12 different nucleosome positioning datasets. Setting 2 (Single stage fine tuning) leads to minimum performance across the CE in terms of accuracy 88.80% and AUC-ROC 94.28%. Whereas, setting 1 (MLM training) achieves higher performance scores as compared to setting 2, with an accuracy score of 89.2%, and AUC-ROC score of 95.0% over CE. Overall, setting 1 achieves better performance scores as compared to setting 1 with a gain of 1.2% across accuracy and 0.72% across AUC-ROC. Setting 3 yields maximum performance scores over the CE dataset as compared to setting 1 and setting 2. Overall, it obtains performance enhancements of 1.3% over the accuracy and 0.8% over AUC-ROC in terms of CE as compared to setting 1.

Over HM dataset, setting 1 produces the lowest performance scores as compared to the other settings i.e., 83.1% accuracy and 91.4% AUC-ROC. In comparison, setting 2 outperforms setting 1 across performance scores related to 4 different evaluation measures, for instance, 4.91% in terms of accuracy. Setting 3 obtains the maximum performance scores across 5 different evaluation measures as compared to setting 2 i.e., 0.3% in terms of accuracy and 3.23% over AUC-ROC. For HS dataset, setting 3 shows more robust and generalizable performance due to no difference in specificity and sensitivity scores, as compared to setting 1 and 2 i.e., 7.5% and 3.71%.

On the dataset of DM, setting 3 shows maximum performance scores across accuracy 85.1%, MCC 70.5%, and sensitivity 84.8%. In comparison setting 2 achieves comparable performance to setting 3, which is better as compared to setting 1 across MCC, AUC-ROC, accuracy, and sensitivity. Whereas, across the dataset of YS, all three settings lead to similar per-

formance over all the evaluation measures. Overall across G1 datasets, except for setting 1, both settings 2 and 3 show better generalizability and robustness for the prediction of samples belonging to positive and negative classes, whereas setting 3 achieves the best and maximum performance on all the datasets.

On the other hand, to validate the claim that setting 3 is the best among all for nucleosome positioning prediction, the evaluation is also performed on 8 different datasets from G2 through 5-fold validation. For DM in G2, setting 1 achieves better performance scores across accuracy and AUC-ROC only over DM-5U dataset with scores of 69.9% and 68.7%, with performance margins across accuracy and AUC-ROC of 0.4% respectively. For DM-LC, setting 3 outperforms setting 1 and setting 2 across accuracy and AUC-ROC i.e., 71.3% and 72.0%, with a gain of 0.5% across accuracy, and 0.4% over AUC-ROC. Similarly, setting 1 and 3 show similar performance over DM-PM across accuracy i.e., 73.6%, yet setting 3 achieves better AUC-ROC with a gain of 0.5%.

Across the datasets of YS, setting 3 achieves maximum accuracy and AUC-ROC. For instance, it achieves accuracy and AUC-ROC scores of 92.4% and 93.5%. Similarly, over YS-WG dataset setting 3 obtains maximum performance across accuracy and AUC-ROC i.e., 94.3% and 94.5%, which are 1.3% and 0.8% better than the maximum accuracy and AUC-ROC scores from setting 1 and setting 2.

Over HM-LC datasets, just like prior mentioned cases, setting 3 gives maximum accuracy and AUC-ROC, which are 0.3% better than that of setting 2. Similarly, the performance scores of evaluation measures over HM-5U reveal that the accuracy and AUC-ROC of setting 3 are 81.8% and 80.2% respectively, which are 0.8% and 0.2% greater than setting 2, respectively. The same trend is observed in the case of HM-PM, where the accuracy of setting 3 is 1.6% better than that of setting 2 while AUC-ROC shows only 0.8% improvement.

Overall, the performance of setting 3 is quite robust and better than setting 1 and 2 over both groups of datasets, therefore it is used for the performance comparison with state-of-the-art and further nucleosome positioning prediction. In addition, as setting 3 is based on two-stage fine-tuning, the additional fine-tuning step helps the BERT model to learn diverse types of nucleosome-related features from the datasets in a better way as compared to setting 1, and 2 of BERT-based architectures.

Table 5: Performance values of 6 evaluation measures across G1 datasets for all nucleosome positioning predictors.

Dataset/Species	Method	ACC	SP	SN	PR	MCC	AUC-ROC	1 st stage training
DM	NP-BERT (Proposed)	85.1	85.6	84.8	85.3	70.5	92.4	YS
	DLNN (Di Gangi et al., 2018)	85.6	83.33	87.0	-	-	-	
	ZCMM (Cui et al., 2019)	93.62	79.64	92.26	-	70.0	91.0	
	NP_Cbir (Han et al., 2022)	85.55	83.37	87.69	-	71.19	92.51	
	CORENup (Amato et al., 2020)	87.0	86.0	87.9	86.1	74.0	93.4	
CE	NP-BERT (Proposed)	90.5	92.1	88.1	91.8	80.5	95.8	YS
	DLNN (Di Gangi et al., 2018)	89.62	86.34	93.04	-	-	-	
	ZCMM (Cui et al., 2019)	85.34	84.1	78.8	-	62.0	91.2	
	NP_Cbir (Han et al., 2022)	89.39	84.59	94.27	-	79.24	95.3	
	CORENup (Amato et al., 2020)	89.5	87.4	93.5	87.4	80.0	95.0	
HM	NP-BERT (Proposed)	88.3	88.4	88.3	88.5	76.8	94.4	CE
	DLNN (Di Gangi et al., 2018)	85.37	82.29	88.3	-	-	-	
	ZCMM (Cui et al., 2019)	77.2	81.51	-	-	56.0	86.1	
	NP_Cbir (Han et al., 2022)	86.12	83.3	89.09	-	72.84	92.34	
	CORENup (Amato et al., 2020)	84.9	81.8	88.8	81.8	70.2	92.2	
YS	NP-BERT (Proposed)	100	99.8	100	99.8	99.8	100	CE
	CORENup (Amato et al., 2020)	99.9	99.8	99.9	99.8	99.8	99.9	
	ZCMM (Cui et al., 2019)	96.75	96.56	91.40	-	88	97.2	

Table 6: Performance values of 6 different evaluation measures of the NP-BERT (Two stage) on the G2 datasets in terms of 5-fold validation.

Datasets	ACC	SP	SN	PR	MCC	AUC-ROC	1 st stage training
DM-5U	69.5	85.8	41.1	63.8	30.8	68.3	YS
DM-PM	73.6	93.6	40.1	80.4	42.0	73.7	YS-PM
DM-LC	71.3	90.0	43.1	75.2	38.7	72.0	YS-PM
HM-5U	81.8	94.3	51.6	80.0	53.4	80.2	YS
HM-LC	91.1	96.1	83.7	93.7	81.7	95.1	CE
HM-PM	85.1	92.4	75.8	89.1	70.1	90.4	YS
YS-PM	92.4	97.2	63.1	79.6	66.3	93.5	YS
YS-WG	94.3	98.4	60.3	82.7	67.2	94.5	YS-PM

5.2 NP-BERT vs State-of-the-Art

The two-stage fine-tuning leads to the maximum performance over nucleosome positioning, so the performance scores of different evaluation measures of 5 existing nucleosome positioning predictors are compared only with the two-stage fine-tuned BERT. Table 5, 6 and 7, show the performance comparison of the proposed BERT for nucleosome position across G1 and G2 datasets in terms of 6 different evaluation measures i.e., accuracy, specificity, sensitivity, precision, MCC, and AUC-ROC

Table 5 contains the performance values of proposed and existing predictors on G1, where the proposed predictor beats the existing predictors in 3 out of 4 datasets. In the case of DM the proposed predictor shows inferior performance to 2 existing predictors, namely ZCMM, and CORENup, where ZCMM

is prone to overfitting due to a difference of 12.62 % in their specificity and sensitivity scores. In comparison, CORENup and the proposed approaches are more generalizable for samples belonging to both classes, due to a lesser difference in specificity and sensitivity scores. For the dataset of CE, the proposed predictor beats all the existing approaches across 4 different evaluation measures. Overall the proposed predictor achieves performance gains of 0.88% across accuracy, 5.76% increase in terms of specificity, a 0.5% increase in terms of MCC, and a 0.8% increase in terms of AUC-ROC. The proposed predictor is more generalizable for positive and negative samples due to less difference in specificity and sensitivity, i.e., 1.6% as compared to existing predictors i.e., 6.74%, 5.3%, 5%, and 2.1%.

Similarly, for the dataset of HS, the proposed method gains performance improvements across 4 different evaluation measures, overall it achieves a performance improvement of 2.2% in terms of accuracy, 5.1% in specificity, 3.96% over MCC, and 2.06% over AUC-ROC. In addition, the proposed predictor has approximately no difference in specificity and sensitivity scores, which again reveals the robustness and generalizability of the model as compared to other predictors where the difference in specificity and sensitivity is comparatively high. For the dataset of YS, CORENup and the proposed predictor reach up to 100% in terms of accuracy and AUC-ROC which means that both the approaches are more suitable for nucleosome positioning across YS datasets.

Table 6 and 7 contain the performance values

Table 7: Performance comparison with state-of-the-art nucleosome positioning predictors across G2 datasets in terms of 5-fold validation.

Dataset/Species	Best for Liu (Liu et al., 2014)	DLNN (Di Gangi et al., 2018)	CORENup (Amato et al., 2020)	NP_CBiR (Han et al., 2022)	NP-BERT (Proposed)
DM-5U	70.0	68.0	69.6	78.0	68.3
DM-PM	70.0	71.0	74.0	74.0	73.8
DM-LC	70.0	71.0	72.0	72.0	72.0
HM-5U	70.0	68.0	76.6	78.0	80.2
HM-LC	65.0	81.0	90.0	92.0	95.1
HM-PM	67.0	77.0	86.0	86.0	90.4
YS-PM	-	83.0	92.9	-	93.5
YS-WG	-	83.0	93.2	-	94.5

of proposed and existing predictors on G2 datasets, where the proposed predictor beats the existing predictors in 5 datasets, shows equivalent performance in 2 datasets, and shows inferior performance across only 1 dataset. Across the datasets of DM, the proposed predictor achieves similar performance on DM-PM and DM-LC datasets and inferior performance on DM-5UT datasets. Whereas, for the datasets of HM, the predictor achieves a performance improvement of 2.2% in terms of AUC-ROC for HM-5UT, a gain of 3.51 % across HM-LC, and an increase of 4.4% over AUC-ROC in HM-PM dataset. Similarly, in terms of YS datasets, the predictor achieves performance enhancement of 0.6% for YS-PM, and 1.3% for the dataset of YS-WG. Overall, the AUC-ROC of the proposed remains comparatively higher than existing methods, which provides evidence for lower bias of the model toward the positive and negative class samples.

The better performance of the proposed approach is associated with efficient and discriminative representations learned from the two-stage fine-tuning. This is evident from the feature space as well, the clusters of positive and negative class samples are independent of each other with some outliers. Due to the superior performance of NP-BERT as compared to multiple SOTA methods across different nucleosome positioning datasets, and low bias for positive and negative samples, therefore it can be considered a more definitive method to predict nucleosome positioning from raw DNA sequences.

5.3 Traditional DNA Feature Extractors VS NP-BERT

In order to analyze the performance of feature extraction methods on nucleosome prediction, an extrinsic performance analysis is performed on all datasets of nucleosome prediction by training and evaluating a random forest (RF) classifier with the obtained statistical feature representations over 5-fold validation.

Table 8 shows, the maximum performance obtained by a feature extraction method and RF classifier. For each dataset only the top-performing fea-

Table 8: Performance values of top performing feature extraction methods for nucleosome positioning datasets.

Dataset/Species	Method	SN	SP	PR	ACC	MCC	AUC-ROC	AUPRC
Group 1								
DM	ENAC	79.89	78.476	78.60	79.18	58.4	86.28	85.98
HM	CKSNAP	81.13	87.68	87.24	84.38	69.09	91.17	91.50
CE	PS2	86.006	85.43	85.762	85.718	71.46	91.9	93.18
YS	DACC	99.88	99.94	99.94	99.91	99.83	100	100
Group 2								
DM-5U	PseEIIIP	35.6	90.61	68.85	70.46	32.29	69.0	61.93
DM-PM	Mismatch	44.6	91.04	74.9	73.71	41.51	72.93	69.08
DM-LC	CKSNAP	44.82	89.88	74.63	71.94	39.84	72.95	70.94
HM-5U	CKSNAP	39.44	95.66	79.55	79.18	45.35	76.9	67.44
HM-PM	K-MER	66.634	92.076	87.09	80.83	61.71	85.84	87.21
HM-LC	RCK-MER	75.10	94.4	90.10	86.62	72.27	91.85	91.53
YS-PM	ENAC	4.05	99.67	67.06	86.274	14.11	81.67	44.67
YS-WG	K-MER	14.05	99.44	75.55	90.18	29.83	86.23	51.09

ture extraction method is shown. The performance achieved by the statistical feature extraction methods is comparatively low as compared to the contextual information dependent i.e., DLNN (Di Gangi et al., 2018), Np_CBiR (Han et al., 2022), and also to the proposed NP-BERT model in terms of all 12 benchmark datasets. In addition, none of the feature extraction methods has consistent performance across multiple nucleosome positioning datasets. This suggests that these feature extraction methods might not be suitable enough to be used to identify nucleosome positioning across multiple species precisely.

As per the performance scores on the G2 datasets, the statistical feature extraction methods along with RF, yield poor performance as the datasets are highly imbalanced. Such imbalanced datasets make the model more biased towards the samples of one class which is obvious from huge sensitivity and specificity differences i.e., >50%. Therefore, using such features becomes more problematic to gain consistent performance across a series of datasets belonging to different species.

To complement the extrinsic performance analysis of the various feature extraction methods, Figure 3 shows the feature space of the statistical representations obtained by applying t-distributed stochastic neighbor embedding (TSNE). Most of the feature extraction methods show heavily dependent clusters among nucleosome forming and linker sequences

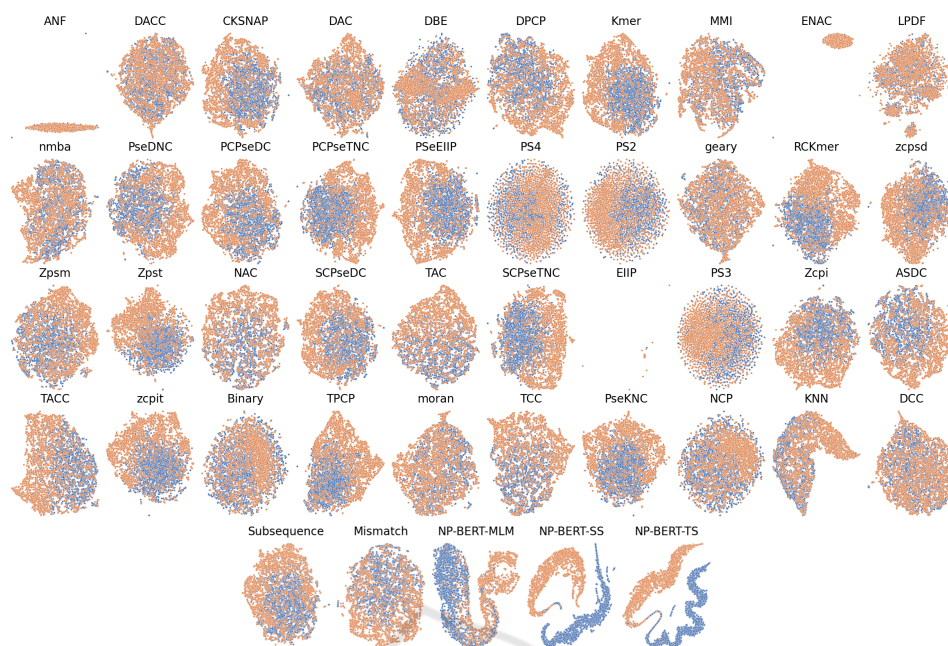


Figure 3: TSNE visualization of different DNA feature extraction methods. NP-BERT-SS represents features from single-stage fine-tuned BERT model, NP-BERT-TS shows features two-stage fine-tuned BERT model, and NP-BERT-MLM shows features from BERT model with MLM training.

(positive and negative samples), which suggests that these methods are unable to encode discriminatory information in the statistical representations. In addition, methods like PseKNC, CKSNAP, Z curve, DAC, and TAC show unique yet dependent clusters which means that overall these methods deliver reasonable performance over nucleosome positioning datasets, yet the performance is lower than the current state-of-the-art nucleosome positioning predictors. This is also apparent from the performance values that are already discussed earlier. In comparison, the features obtained by the BERT-based models (NP-BERT) produce independent and unique clusters for the samples belonging to positive and negative classes, which prove the discriminatory power and efficiency of the proposed approach for nucleosome positioning prediction.

6 CONCLUSION

In this research, a transformers-based deep learning model for the identification of nucleosome positioning across multiple species is presented. The proposed approach is tested in three different experimental settings to explore the potential of transfer learning and BERT pre-training for nucleosome positioning. Comparative performance analysis is performed that

shows that setting 3 leads to maximum performance on nucleosome positioning datasets. Moreover, the performance produced by setting 3 is then compared with state-of-the-art deep learning models and multiple statistical feature extraction methods. The proposed predictor beats the statistical DNA feature extraction methods across all the datasets, whereas it beats the state of art deep learning models across 3 out of 4 nucleosome positioning G1 datasets, 5 out of 8 G2 datasets across 5-fold validation, and shows equivalent performance on 2 G2 datasets. Overall, the performance gains obtained by the proposed predictor range from 0.88% to 2.2% across accuracy, 0.10% to 2.1% in terms of AUC-ROC, over G1 datasets. Similarly, for G2 datasets the gains vary from 0.6% to 4.4% in terms of AUC-ROC over 5-fold validation. In addition, NP-BERT shows consistent performance across the majority of the datasets which makes it more suitable than other approaches for the prediction of nucleosome positioning. The proposed approach can help the scientific community with more accurate analyses of nucleosome positioning and gene regulation. Furthermore, this work can be extended by incorporating an ensembling strategy at setting 3 which can provide further performance gains, and also this methodology can be tested out for multiple other challenging genome classification tasks.

REFERENCES

- Amato, D., Bosco, G., and Rizzo, R. (2020). Corenup: a combination of convolutional and recurrent deep neural networks for nucleosome positioning identification. *BMC bioinformatics*, 21(8):1–14.
- Buenrostro, J. D., Wu, B., Chang, H. Y., and Greenleaf, W. J. (2015). Atac-seq: a method for assaying chromatin accessibility genome-wide. *Current protocols in molecular biology*, 109(1):21–29.
- Chen, R., Kang, R., Fan, X., and Tang, D. (2014). Release and activity of histone in diseases. *Cell death & disease*, 5(8):e1370–e1370.
- Chen, W., Feng, P., Ding, H., Lin, H., and Chou, K.-C. (2016). Using deformation energy to analyze nucleosome positioning in genomes. *Genomics*, 107(2-3):69–75.
- Chen, Z., Zhao, P., Li, C., Li, F., Xiang, D., Chen, Y.-Z., Akutsu, T., Daly, R. J., Webb, G. I., Zhao, Q., et al. (2021). ilearnplus: a comprehensive and automated machine-learning platform for nucleic acid and protein sequence analysis, prediction and visualization. *Nucleic acids research*, 49(10):e60–e60.
- Cheraji, R. V. and Clark, D. J. (2018). Major determinants of nucleosome positioning. *Biophysical journal*, 114(10):2279–2289.
- Cho, K. S., Elizondo, L. I., and Boerkoel, C. F. (2004). Advances in chromatin remodeling and human disease. *Current opinion in genetics & development*, 14(3):308–315.
- Cui, Y., Xu, Z., and Li, J. (2019). Zcmm: A novel method using z-curve theory-based and position weight matrix for predicting nucleosome positioning. *Genes*, 10(10):765.
- Devlin, J., Chang, M.-W., Lee, K., and Toutanova, K. (2018). Bert: Pre-training of deep bidirectional transformers for language understanding. *arXiv preprint arXiv:1810.04805*.
- Di Gangi, M., Lo Bosco, G., and Rizzo, R. (2018). Deep learning architectures for prediction of nucleosome positioning from sequences data. *BMC bioinformatics*, 19(14):127–135.
- Floridi, L. and Chiriatti, M. (2020). Gpt-3: Its nature, scope, limits, and consequences. *Minds and Machines*, 30(4):681–694.
- Han, G.-S., Li, Q., and Li, Y. (2022). Nucleosome positioning based on dna sequence embedding and deep learning. *BMC genomics*, 23(1):1–11.
- Huang, Y., Niu, B., Gao, Y., Fu, L., and Li, W. (2010). Cd-hit suite: a web server for clustering and comparing biological sequences. *Bioinformatics*, 26(5):680–682.
- Ji, Y., Zhou, Z., Liu, H., and Davuluri, R. V. (2021). Dnabert: pre-trained bidirectional encoder representations from transformers model for dna-language in genome. *Bioinformatics*, 37(15):2112–2120.
- Koumakis, L. (2020). Deep learning models in genomics; are we there yet? *Computational and Structural Biotechnology Journal*, 18:1466–1473.
- Liu, H., Zhang, R., Xiong, W., Guan, J., Zhuang, Z., and Zhou, S. (2014). A comparative evaluation on prediction methods of nucleosome positioning. *Briefings in bioinformatics*, 15(6):1014–1027.
- Luger, K. (2003). Structure and dynamic behavior of nucleosomes. *Current opinion in genetics & development*, 13(2):127–135.
- Mikolov, T., Sutskever, I., Chen, K., Corrado, G. S., and Dean, J. (2013). Distributed representations of words and phrases and their compositionality. *Advances in neural information processing systems*, 26.
- Muhammad, R., Ahmed, S., Md Farid, D., Shatabda, S., Sharma, A., and Dehzangi, A. (2019). Pyfeat: a python-based effective feature generation tool for dna, rna and protein sequences. *Bioinformatics*, 35(19):3831–3833.
- Ozsolak, F., Song, J. S., Liu, X. S., and Fisher, D. E. (2007). High-throughput mapping of the chromatin structure of human promoters. *Nature biotechnology*, 25(2):244–248.
- Peckham, H. E., Thurman, R. E., Fu, Y., Stamatoyannopoulos, J. A., Noble, W. S., Struhl, K., and Weng, Z. (2007). Nucleosome positioning signals in genomic dna. *Genome research*, 17(8):1170–1177.
- Pedregosa, F., Varoquaux, G., Gramfort, A., Michel, V., Thirion, B., Grisel, O., Blondel, M., Prettenhofer, P., Weiss, R., Dubourg, V., et al. (2011). Scikit-learn: Machine learning in python. *the Journal of machine Learning research*, 12:2825–2830.
- Sakketou, F. and Ampazis, N. (2020). A constrained optimization algorithm for learning glove embeddings with semantic lexicons. *Knowledge-Based Systems*, 195:105628.
- Schmid, C. D. and Bucher, P. (2007). Chip-seq data reveal nucleosome architecture of human promoters. *Cell*, 131(5):831–832.
- Shtumpf, M., Piroeva, K. V., Agrawal, S. P., Jacob, D. R., and Teif, V. B. (2022). Nucposdb: a database of nucleosome positioning in vivo and nucleosomics of cell-free dna. *Chromosoma*, 131(1):19–28.
- Tsompana, M. and Buck, M. J. (2014). Chromatin accessibility: a window into the genome. *Epigenetics & chromatin*, 7(1):1–16.
- Ulianov, S. V., Khrameeva, E. E., Gavrillov, A. A., Flyamer, I. M., Kos, P., Mikhaleva, E. A., Penin, A. A., Logacheva, M. D., Imakaev, M. V., Chertovich, A., et al. (2016). Active chromatin and transcription play a key role in chromosome partitioning into topologically associating domains. *Genome research*, 26(1):70–84.
- Yu, Y., Si, X., Hu, C., and Zhang, J. (2019). A review of recurrent neural networks: Lstm cells and network architectures. *Neural computation*, 31(7):1235–1270.
- Zhang, J., Peng, W., and Wang, L. (2018). Lenup: learning nucleosome positioning from dna sequences with improved convolutional neural networks. *Bioinformatics*, 34(10):1705–1712.